Chapter 7

Optical Pressure Measurement Principle System

Limin Gao, Ruiyu Li and Bo Liu

Additional information is available at the end of the chapter

http://dx.doi.org/10.5772/64008

Abstract

Surface pressure measurements are critical to aerodynamic testing in wind tunnel. A new pressure measurement technique is being developed to augment current capabilities that are an optical-based technique using pressure sensitive paint (PSP). Compared with the traditional surface pressure measurement, an important feature of optical pressure measurement is much more complete surface information with relatively simple procedures and instrumentation. So optical pressure measurement technique will provide an alternative to conventional methods for the pressure measurement. After studying the chapter of "Optical Pressure Measurement System", readers are expected to grasp the measurement principle and know how to establish the corresponding measurement system. In this chapter, the measurement principle, measurement system, component characteristics and its application of optical pressure measurement technique are introduced based on the authors' research.

Keywords: surface pressure, pressure sensitive paint, optical pressure measurement

1. Introduction

Surface pressure measurements are critical to aerodynamic testing in wind tunnel. For experimental research, pressure has often been measured for its ability of revealing complex flow phenomena such as shock wave, boundary layer separation, etc.

Conventional pressure measurement method is based on pressure taps and electronically scanned pressure transducers. Pipes connect these holes to pressure transducers, which transform the mechanical force of the pressure to a digital or analogy reading. Since the effective area for a single tap is rather limited, there could be several large arrays of hundreds or even thousands of pressure taps to be employed in industrial wind tunnel testing. Although

these devices provide accurate pressure information, depending on the size and complexity of the model, the process of creating these models is time-consuming and expensive, while the preparation for wind tunnel testing is rather tedious and laborious. Thus it is the first drawback that using a pressure tap system needs much cost in time and labour and money. The other drawbacks include the fact that the number of taps should be limited because of the minimum space between pressure taps which lead to poor space resolution and the taps would introduce aerodynamic interference in wind tunnel testing which might affect the total pressure profiles along the pressure model surfaces as well as the difficulties of taps drilling and pipe arrangement on the surfaces with thin structures.

A new pressure measurement technique has been developed to augment the conventional surface pressure measuring method in aerodynamic testing, which actually is an optical-based technique using pressure sensitive paint (PSP). Compared to the conventional pressure measurement method, PSP technique provides a relatively simple and inexpensive way to acquire full-field pressure image on aerodynamic model surface with high spatial resolution and low aerodynamic interference resulting from PSP coating. Since it is with both functions of flow visualization and flow field measurement, PSP technique could reflect the details of flow structure on model surfaces such as traces of vortices, flow separation and reattachment and shock waves. The process of model-making and testing preparation is easy to manipulate with less time and less expense. PSP model needs less number taps for in-situ calibration and even the aerodynamic force model could be employed to acquire surface pressure distribution by PSP technique. If two-dimensional pressure data is mapped onto the three-dimensional model surface, aerodynamic force can be obtained by integration over the model surface.

PSP technique introduces an innovative concept of instrumentation and provides entire surface pressure map with high spatial resolution. In recent years, surface pressure distribution measurement technique using pressure sensitive paint (PSP) has been recently receiving popularity in the aerospace fields. The central Aero-Hydrodynamic Institute (TsAGI) [1,2] in Moscow, NASA [3–6] and McDonnell Douglas Aerospace (MDA) [7] are the PSP pioneers who published some PSP application results in wind tunnel, and the studied area includes the pressure distributions on the Delta-wing, the iced wing, the cooled film as well as famous combat fighter and civil transporter such as F-16, F-18 and several Boeing and Air Bus transporters. So far the convenient commercial PSP measurement system has been developed by ISSI (Innovative Scientific Solution Inc.). So Optical Pressure Measurement technique will act as an alternative to conventional methods for the pressure measurement.

2. Measurement principle

This section briefly reviews luminescence and quenching as it pertains to pressure sensitive paint. The image-based PSP technique is an optical method that enables measurements of surface pressure distributions over a model. More detailed discussions of these phenomena can be found in textbooks, for example, by Willard et al., Tianshu Liu.

http://dx.doi.org/10.5772/64008

Pressure sensitive paint techniques are based on photoluminescence (which includes both fluorescence and phosphorescence) of some polymer probe molecules, as shown in **Figure 1.** When photons of particular wavelength impinge on the model surface with PSP coating, the probe molecule is promoted to an excited state by absorbing photons with appropriate energy. Then immediately excited probe molecule must return to the ground state by emitting photons of a longer wavelength to lose the excited energy. This process is called photoluminescence. Meanwhile, there exists other ways for excited molecules to lose energy, one of which is the process to transfer much excited energy to oxygen molecules penetrating into PSP coating by colliding and to decrease the emitting intensity, named as oxygen quenching. The working process of PSP involves those of photoluminescence and quenching, denominated as Stern-Volmer process, in which the intensity of PSP is inversed to the concentration of oxygen molecules.

Since the concentration of oxygen molecules in air is always consistent with 21% and that locally inside PSP coatings is proportional to the local pressure outside the coatings, locally low-pressure regions on the surface of a model will emit higher intensity with less quenching than locally high-pressure areas. Thus, pressure can be measured by oxygen quenching of luminescence.

Based on above mentioned photochemical characteristic of PSP, the working process can be modelled by a simplified form of the Stern-Volmer relation as:

$$\frac{I_{ref}}{I} = A(T) + B(T)\frac{P}{P_{ref}} + C(T)(\frac{P}{P_{ref}})^2 + \ldots \tag{1}$$

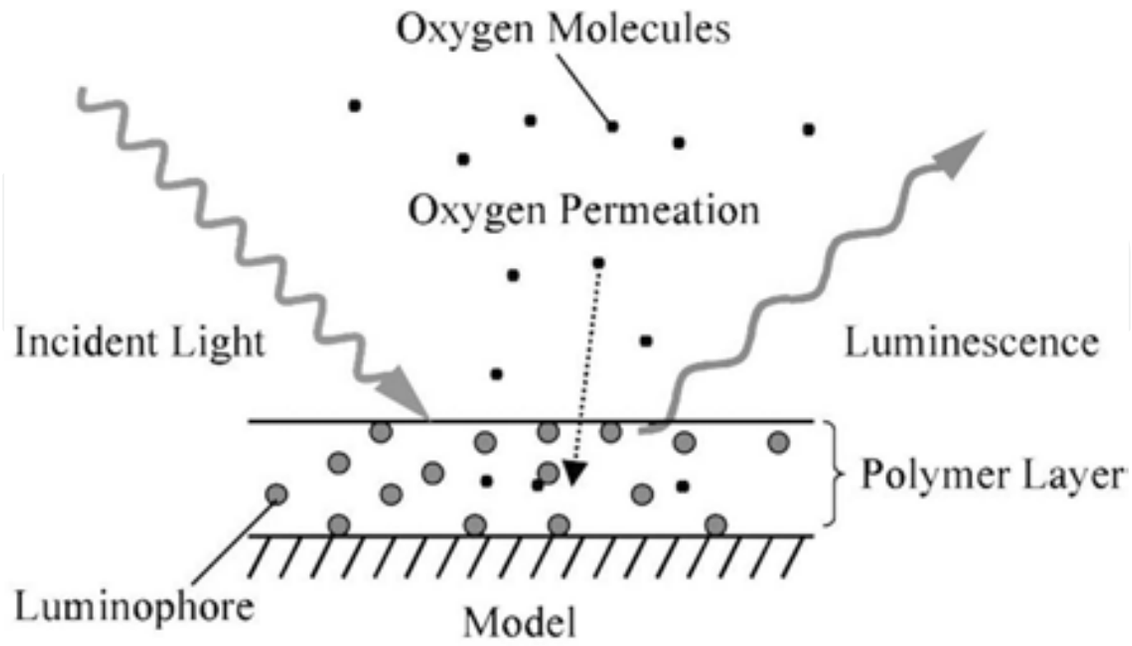

Figure 1. Principle of optical PSP techniques.

Where $I$is the PSP luminescence emitted at the pressure P and I_{ref} is the reference luminescence at a reference pressure P_{ref}. Usually the wind-off condition is selected as the reference condition. The coefficients A and B display the dependence of PSP on the temperature T, which are determined from pre-calibrating tests to be carried out in advanced and related with the paint's formulations. If the paint is insensitive to thermal changes, the coefficients A and B are both constant.

The preconditions for application of PSP technique are so strict and ideal that could never be achieved in practice. First, the uniform luminance on measured surfaces of model, consistent thickness of paint coatings and the distribution of temperature on measured surfaces must be kept the same. Furthermore, relative motion in position and structure distortion during operation should be prohibited, and ideal emission without spectral variability and filter leakage and the rest should be met.

The most popular type of PSP technique is intensity-based method which acquires surface pressure distribution from the ratio image of intensity image at non-operation (wind-off) condition to that at operation (wind-on) by interpolated with pre-established Stern-Volmer equation. In most cases, some pressure taps values are essential and necessary to calibrate and validate PSP data, which process denoted as in-situ calibration. The intensity images are captured by scientific grade CCD or CMOS cameras which are either coloured or greyed type. Although the coloured camera only has one-fourth effective resolution of greyed one with the same nominal resolution, the former camera can provide at least two intensity image at same time. That is to say, the output of either camera is in grey level.

3. Measurement systems

The PSP measurement system should first be compatible to a particular test facility. The portable instruments or devices are necessary. Compatibility of a PSP measurement system to several test facilities is preferred. If compatibility is impossible, a flexible PSP measurement system should be established for cost-efficient purpose. The involved instruments or devices should be of high quality and of perfect performance. Thus the expense to establish PSP measurement system is not too low. An accurate PSP measurement system includes paint formulation, painting device, excited light source, scientific grade camera, calibration devices, image-processing device and software, and other auxiliaries such as filters etc. A perfect PSP measurement system has normally been promoted from an initially primary measurement system. Experience and expertise would play a critical role in the process of PSP measurement system establishment. Primary instruments or devices such as excited light source, calibration devices, image-processing software and filters should be customized, among which the selection of excited light source and filters depends on the spectral performances of paint formulations. The control devices will play an important role in multi-excited sources-and-cameras system. In addition, real time image processing is a perfect aim for PSP measurement system. A sketch of one PSP system configuration used in this investigation is shown in **Figure 2**.

http://dx.doi.org/10.5772/64008

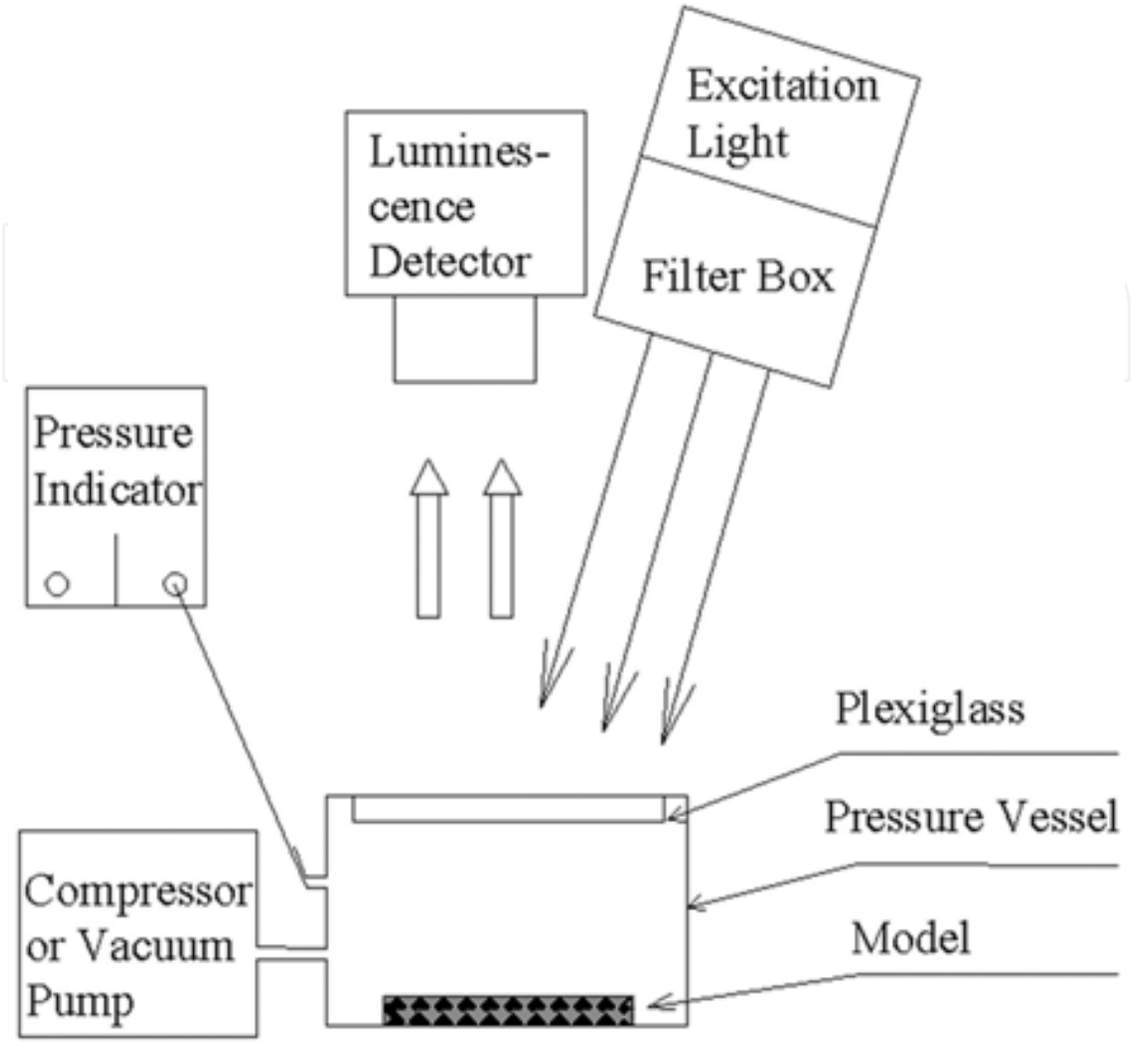

Figure 2. Components of optical PSP measurement system.

3.1. PSP paint layer application

Detailed discussion of the PSP paint formulations are out of the chapter's focus and only briefly described here.

A typical pressure-sensitive paint (PSP) is composed of two main components: oxygen-sensitive fluorescence molecules (which is called the luminescent probe molecules) and oxygen-permeable binder materials. From publications, PSP composed of pyrene or PtTFPP with oxygen-permeable silicon binder are popular in wind tunnel testing, the former of which exists an absorbing peak near 320 to 340 nm among an exciting range from 320 to 390 nm and an emission peak near 440 to 520 nm, the latter of which is excited near 400 nm and then emits a main peak near 650 nm. The pyrene-based paint is developed by ICAS (Institute of Chemistry, Chinese Academy of Science), is insensitive to thermal changes when ambient temperature is below 40°C. Therefore, the spectral characteristic of the used PSP paint should be acquired by the calibration for measurement accuracy.

Figure 3. Cleaning surface with acetone.

Figure 4. Spraying the paint on the surface.

http://dx.doi.org/10.5772/64008

Fine paint application is the basis of PSP measurement which needs specific expertise and experience. There are several steps for operation. First is to remove oil dots, dust and other dirt spots on the model surface needed paint applying with alcohol or acetone (as shown by **Figure 3**). Any surface imperfections that are unwanted should be corrected prior to a final cleaning. Once the model is completely cleaned, model parts that are not to be painted are covered with tape and/or paper. This step assures the surface to be absolutely clean. Second is to spray base coat or primer coating with an air brush on the cleaned model surface and then to cure the primer coating by lifting ambient temperature for several hours or at ambient temperature for more than 12 h. To finish, the cured primer coating with fine sand papers 800–1500 grit. Finishing will promote the uniform coating thickness and enhance the reflection of excited and emission light. Then remove finished dust attached on the coating by spraying mixture of air and acetone. Third is to spray upper coating containing probes molecules as seen in **Figure 4**. The primer coating is over-sprayed with a saturated solution of probe molecule in toluene or acetone. Several over-spray coats are continued until an even colour (deep pink from ISSI or sky blue from ICAS, seen in **Figure 5**, which is dependent on the PSP formulation) is obtained. And then cure it as the same process as the second step. Fourth is to arrange markers on the cured coating for image alignment which will be described in the following section.

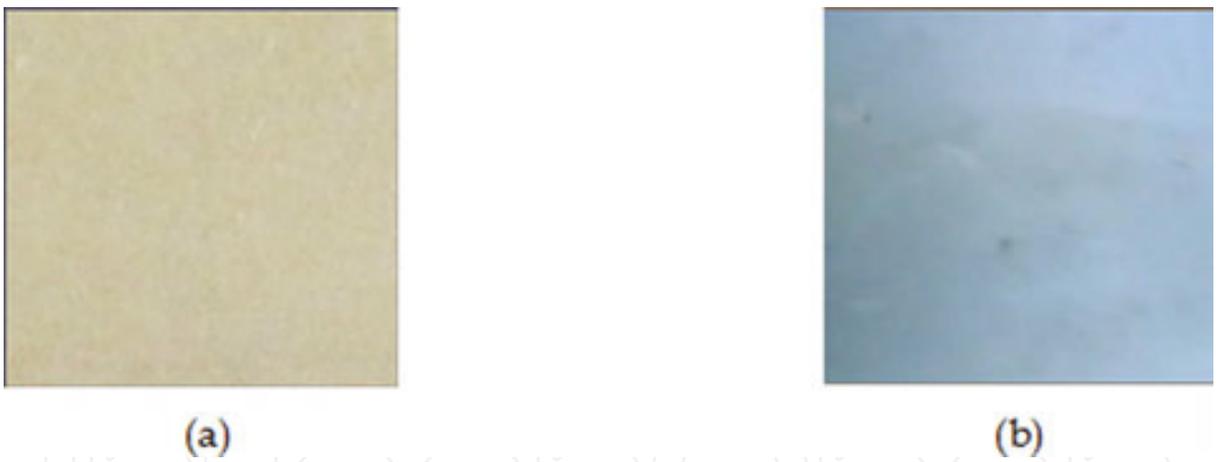

Figure 5. Surface coated with PSP. (a) Paint from ISSI; (b) paint from ICAS.

The paints are applied using a commercial automotive type spray air brush (**Figure 6**) and clean, dry, regulated service air (**Figure 7**). A high volume low pressure (HVLP) touch up sprayer has produced excellent results. Here, the nitrogen is suggested for sprayer instead of the air to avoid the interaction from the oxygen. HVLP sprayers have become standard with their compliance with environmental standards. Jet pressure and area of the sprayer is regulated according the performance of the paint layer. Paint should be sprayed in an area with adequate ventilation. Personal protective equipment must be used depending on the materials being sprayed and the location where the paint is applied.

Figure 6. Spraying air brush (W-71G).

Figure 7. Oil and water filtering regulator for spraying air brush.

http://dx.doi.org/10.5772/64008

3.2. Excitation light source

Pressure sensitive paint working process is denoted as Stern-Volmer process as mentioned previously. The purpose of the excitation light source is to excite the photo luminescent probe molecules. The source must provide an adequate number of excitation photons within appropriate wavelengths. The excited source should avoid emitting photons with wavelength overlap incident photons. Otherwise, Signal Noise Ratio (SNR) of scientific grade camera will decrease to very low level. A range of illumination sources have been considered including lasers, filtered arc lamps, and LED, etc. Here, UV lamp and LED are tested and used.

1. UV lamp

Based on the feature of the paint layer from ICAS, a Porta-Ray 400 portable ultraviolet (UV) lamp made by Uvitron International Company in the U.S. is chosen in the current work, which is a 400W/200W, 1000 h lifetime metal halide lamp. It can emit visible light in a broad spectrum and the maximal output intensity is up to 500 MW/cm^2 within UVA range, whose practical output instability is less than 5%, especially less than 1% after running 30 min.

Additionally, a filter box (**Figure 8**) was designed and manufactured to filter visible light and select UVA light to excite the probe molecules, which consists a metal box, a scattered quartz glass and two pieces of UVA transparent glasses filter. With a pair of latches, the filter box is connected with the UV lamp to form the integrated excitation light source.

Figure 8. UV lamp and filter box.

2. LED arrays

The arrays consists of 37 individual LED (light emitting diode) elements (3W) arranged on a 9.0 cm diameter aluminium substrate and is equipped with water cooled equipment (**Figure 9**) to insure pure illuminating light. The LED array produces light centred at 365 nm (~20 nm full width at half maximum) which is the optimal excitation wavelength. The uniformity of the spot area is beyond 92% with irradiation height of 120 mm. The LED arrays are operated using a 300W switching power supply and can be remotely operated using standard TTL pulse or with continues irradiation mode.

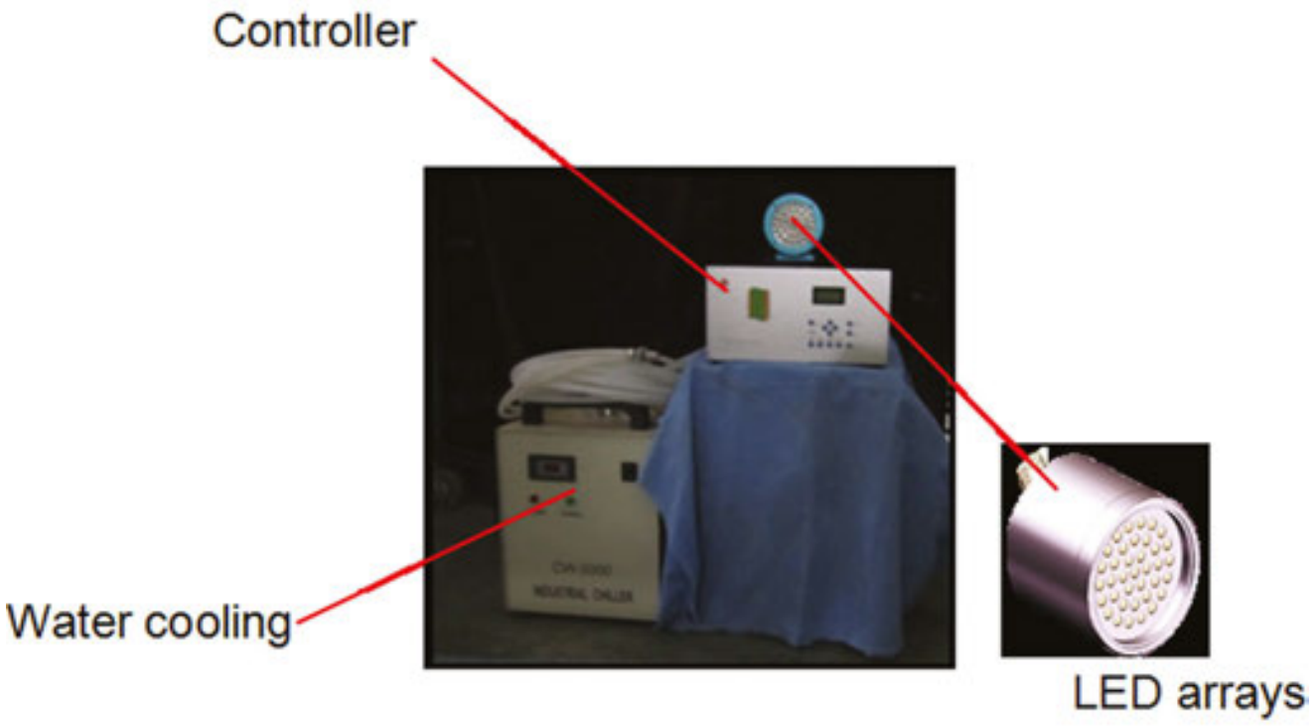

Figure 9. Photo of LED arrays and controller.

3.3. Luminescence detector

Considering the higher readout noise and nonlinear response at low intensity situation, industrial CCD or CMOS camera generally is not fit for accurate PSP measurement. This leads to generation of relatively low SNR (Signal-To-Noise Ratio) Image to decrease its quality. In general, scientific grade CCD or CMOS camera is preferred because its readout noise has been well controlled, and linear response to low intensity has been carefully corrected to satisfy the request of PSP measurement.

In initial study, a TSI charge-coupled device camera (CCD, 1600×1200 pixels, 10 bit) from a Stereo PIV system is chosen as the luminescence photo detector. The image sample is controlled by PIV operating software, INSIGHT 6.0, automatically.

http://dx.doi.org/10.5772/64008

In current study, PSP luminescent emission data is acquired by a specialized air cooled scientific charge-coupled device (CCD) ORCA-R2 camera. A combination of a 24–85mm Nikon zoom lens and 480 nm band pass filter is used in front of the CCD to block excitation. This low noise device allows for the rapid collection of image pairs with a minimal time delay between images. The camera employs a CCD chip with an active area of 1344×1024 pixels with 0.008 ms exposure time and its quantum efficiency is greater than 70% at the wavelength range of 450 nm to 600 nm, which covers the (480 ± 20) nm emission from PSP, and more than 50% near 650 nm. The camera employs 16-bit digital resolution as well as on-board memory that will allow it to rapidly store images; also it provides the high-dynamic range model at 8×8 binning readout if necessary.

3.4. Calibration device

In order to maintain the accuracy of PSP measurement, a calibration device was designed and manufactured, which integrates pressure and temperature adjustors with adequate precision as well as a mediate pressure air pump and an integral cooler and heater. Calibration vessel was customized, which is a steel cylinder with 100 mm diameter ×100 mm high × 8 mm thick and attached with a shrouding ring 20 mm wide atop the plate (**Figure 10**). It is covered with a piece of quartz glass or Plexiglas and connected with a pair of holes as inlet and outlet. With the help of a pressure or vacuum pump, the gas pressure in the pressure vessel can be adjusted 0–200kPa through a pressure manometer.

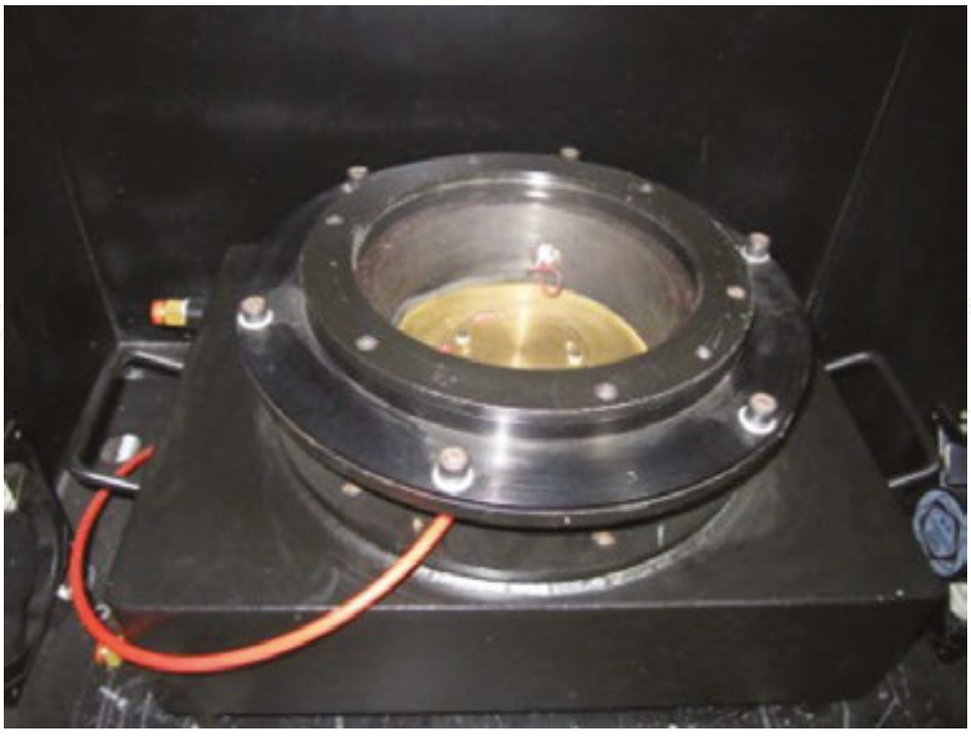

Figure 10. Photo of pressure vessel.

3.5. Image processing

Image processing is a critical step in the whole optical PSP measurement. The current image processing is divided into three parts as shown in **Figure 11**: basic data processing, image registration and 3D reconstruction [8].

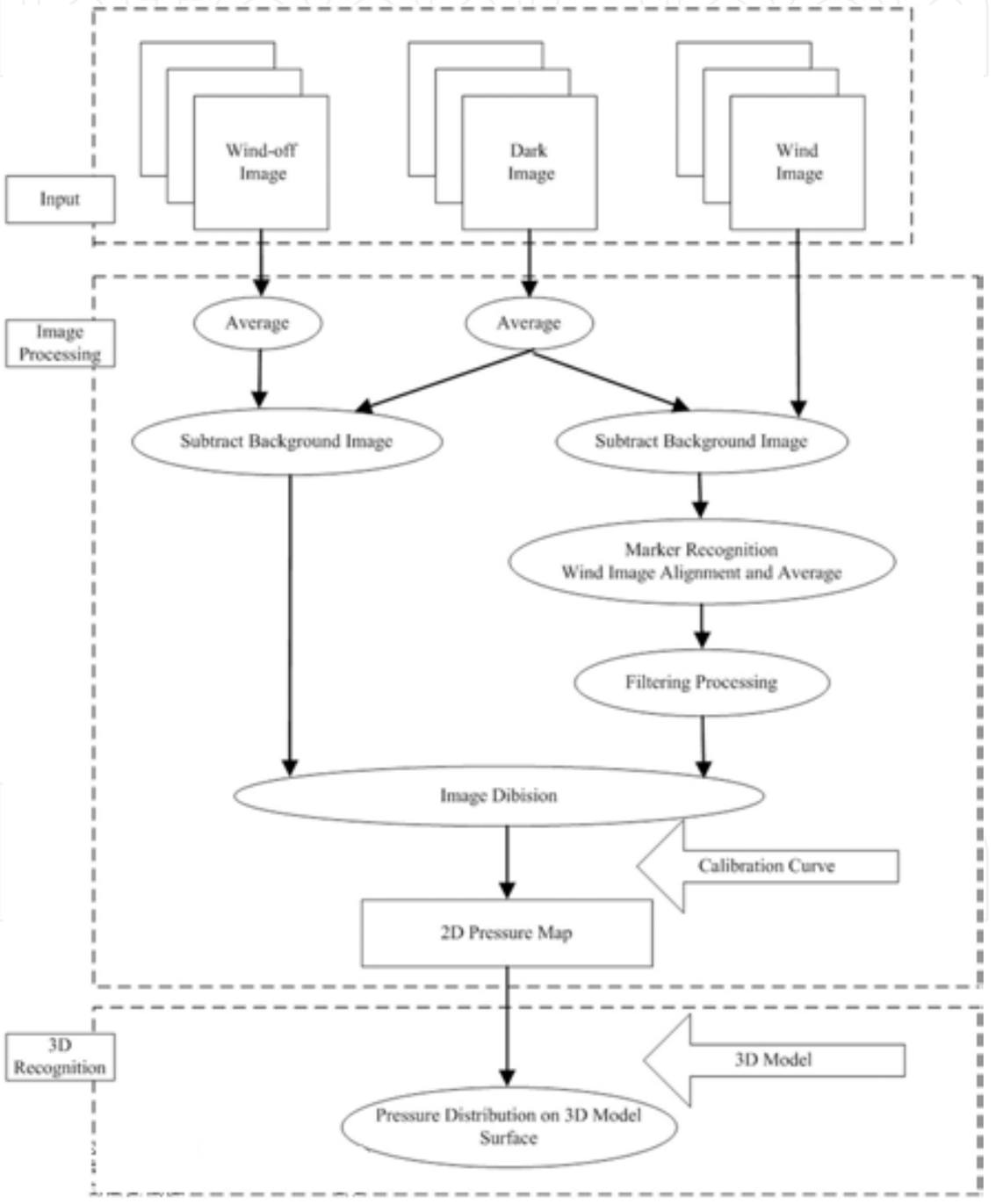

Figure 11. Schematic representation of major steps in PSP data processing.

http://dx.doi.org/10.5772/64008

1. Basic data processing

Transformation from ratio image to pressure map is manipulated with Stern-Volmer Eq. (1) in which Stern-Volmer constants have been determined through a priori calibration. The luminescence I and I_{ref} are intensity images captured at wind-on and wind-off respectively. According to Stern-Volmer equation and by introducing the ambient pressure P_{ref}, a pressure map of model surface can be produced initially.

Generally, the condition of wind-off and wind-on is denoted non-operation and operation of the wind tunnel. It is clear that wind-off means reference condition in Stern-Volmer Eq. (1).

It should be mentioned that the number of images captured at wind-off and wind-on depends on the performances of PSP measurement system, environment and operation condition of the wind tunnel. Besides, a number of dark images and background images should be captured before and after operation respectively. The random noise such as photon shot noise etc. should be restrained by averaging the respective images. The algorithms to suppress the noise generated in image calculations should be chosen carefully because most of them would decrease the effective resolution of selected images.

2. Image registration

In practice, the model surface could move or distort during operation of wind tunnel due to aerodynamic loads and vibrations. Thus, there exist space displacement, structure bending and structure torsion in operation. The situations introduce the difficulties in image ratio calculation due to displacement and structure variation. Hence, image registration must be employed to solve this problem. The wind-on image may not align with the wind-off image due to model deformation produced by aerodynamic loads. **Figure 12(a)** displays an unregistered intensity ratio image of a compressor cascade suction surface, which shows a shadow near each pressure port, as well as two strip-like shadows along leading and trailing edges. The occurrence of shadows might be ascribed to not aligning of wind-on and wind-off images. A ratio between those non-aligned images can lead to a considerable error in calculation of pressure using a calibration relation. Significant errors are introduced if these effects are not included, particularly in regions of rapid pressure changes such as near shock waves, boundary layer transition and flow separation.

To match the deformed pressure image coordinates (x, y) with the reference images coordinates (x_{ref}, y_{ref}), the generalized equation for image registration of image matrices with an $n \times n$ array could be used:

$$\left.\begin{aligned} x_{ref} &= \sum_{i,j=1}^{n} a_{ij} f_i(\mathrm{x}) f_j(y) \\ y_{ref} &= \sum_{i,j=1}^{n} b_{ij} f_i(\mathrm{x}) f_j(\mathrm{y}) \end{aligned}\right\} \tag{2}$$

Figure 12. Image of unregistering (a) and registered (b).

Where both basic functions $f_i(x)$ and $f_j(y)$ are the orthogonal functions or the non-orthogonal power functions $f_i(x) = x_c$ or $f_j(y) = y_c$ with c being a constant value. With the help of the marker recognition and given the image coordinates of alignment reference markers on the measured surface, the unknown coefficients a_{ij} and b_{ij}, can be determined by least-squares fit to match the targets in reference images to those in pressure ones, that keeps the wind-on image locating on the same position as the wind-off image. A registered ratio image is created using the pair of averaged wind-off image and the averaged registered wind-on image. Moreover, the median filtering is performed to reduce the random fluctuation (noise). **Figure 12(b)** shows an aligned intensity ratio image without any shadows. Then the pressure map on the test model is finally revealed as a two dimensional image according to the in-situ calibration curve.

3. 3D reconstruction

In fact, it is very common that the axis of camera lens is not perpendicular to the surface of interest. Thus, 2D pressure map would not provide detailed useful information when normal direction of captured images is not parallel to that of the interest surface. In special case such as testing in cascade wind tunnel, the image is rather distorted and unable to provide more detail on interest surface. To reproduce the pressure map on the 3D test model, 3D reconstructing method is developed based on the projective theory of photogrammetry [9–11].

The perspective relationship between the coordinate (x, y) on the 2D image and (X, Y, Z) on the 3D test model is shown in **Figure 13**. Neglecting the deformation of camera lens, the direct linear transform formulation between 3D test model and 2D image can be expressed by:

$$x = \frac{L_1X + L_2Y + L_3Z + L_4}{L_9X + L_{10}Y + L_{11}Z + 1}$$
$$y = \frac{L_5X + L_6Y + L_7Z + L_8}{L_9X + L_{10}Y + L_{11}Z + 1} \quad (3)$$

http://dx.doi.org/10.5772/64008

Figure 13. Perspective between 2D image and 3D model.

With the help of the over six marks, the transforming coefficient $L_1 \sim L_{11}$ can be solved. Then pressure information on the 2D image is transformed to the 3D model directly without any

loss. The pressure map on the 3D test model is expressed in a stereo vision, and more flow details are provided for engineer. The whole flowchart of 3D reconstruction is given in **Figure 14**.

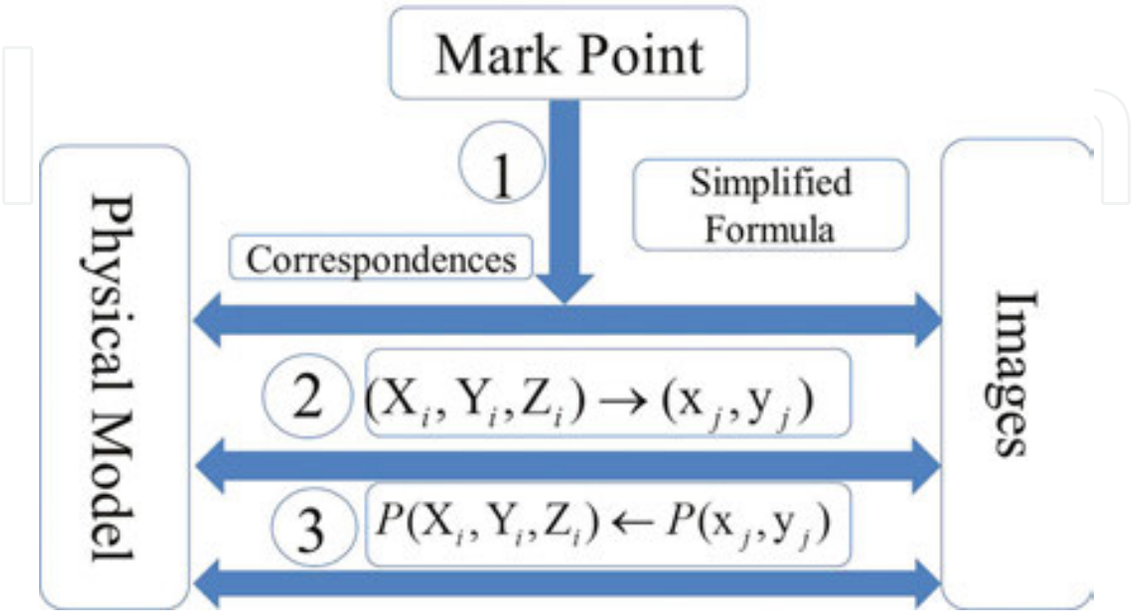

Figure 14. Flow chart of 3D reconstruction.

4. Study of PSP measurement system characteristics

When a set of PSP measurement system has been established, it should be corrected and validated via several PSP calibrations using mature PSP formulation. This is the basis for practical PSP applications.

Having established the PSP measurement system, the validation of its performances and the investigation of selecting relevant system parameters have been conducted in Laboratory of Aerofoil & Cascade Aerodynamics, Northwestern Polytechnical University (NPU). More detailed work has been published in the reference [12,13]. During the calibration process, it is kept dark in the ambient to avoid lighting contamination.

A sample coated with the paint layer is placed in the pressure calibration vessel bottom, which is about 50 mm×50 mm. According to a cascade transonic wind tunnel, the pressure calibration range is determined from 27.4 kPa to 217.4 kPa with interval 10 kPa. To optimize the measurement system, the calibration experiment is performed with five apertures of CCD (2.8, 4, 5.6, 8 and 11) and two powers of UV lamp (200*W* and 400*W*). To reduce the noise of the camera, a total of 20 sequential images are sampled and ensemble-averaged on the same measuring condition

http://dx.doi.org/10.5772/64008

4.1. Excitation characteristics of light source power

Figure 15 shows the original PSP images under typical pressures using two power settings of UV lamp on the condition that the camera aperture is 2.8. There is an inverse relationship between the emitted light intensity and the local air pressure according to the oxygen quenching characteristics of the PSP. Thus, with the pressure increasing, the image is getting darker as shown in **Figure 15**, which is in agreement with the principle of PSP technique. Furthermore, it is very clearly observed by naked eyes that the image **Figure 15(b)** using 400*W* UV lamp is a little brighter comparing with **Figure 15(a)** using 200*W*.

To show the difference between **Figure 15(a)** and (b) more clearly, the luminous intensity of the image is quantified using the grey value of the model surface centred point in **Figure 16**. The luminous intensity using 400*W* UV lamp in **Figure 16(b)** is obviously greater than using 200*W* in terms of the grey scale. When the air pressure in the pressure vessel is 217.4 *kPa*, the luminous intensity using 400*W* UV lamp is I=0.175, but I=0.0717 using 200*W*. Additionally, **Figure 16(b)** shows better linearity with the pressure increase, but sampled points in **Figure 16(a)** are scattered due to low SNR. The main reason is that the energy of the excitation light is relatively weak with 200*W* UV lamp and can't provide the adequate excitation photons to excite fluorescence molecules entering the energy transition.

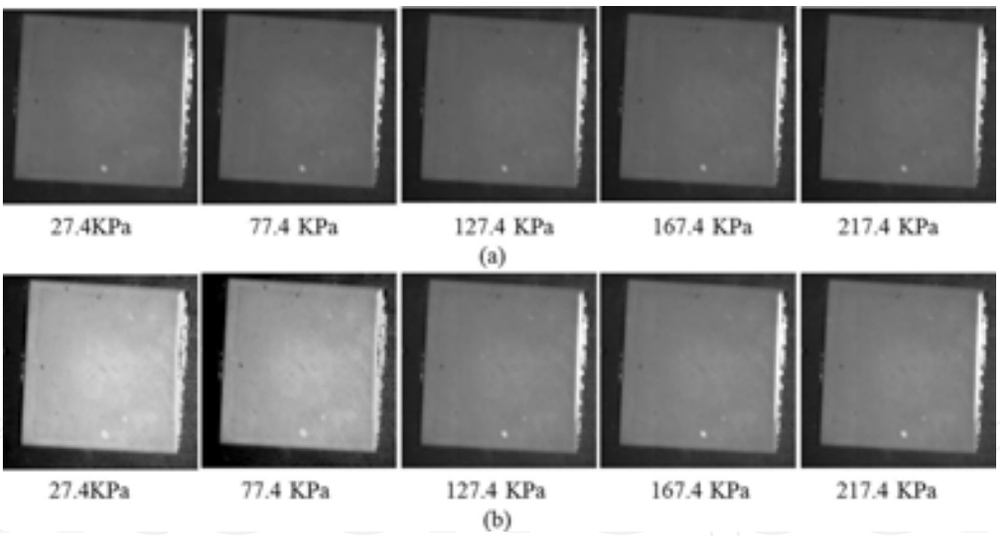

Figure 15. Images using two powers of UV lamp. (a) 200W power; (b) 400W power.

Figure 17 shows the PSP calibration curves using both 200*W* and 400*W* UV lamp on the condition that typical apertures are 2.8, 5.6 and 11, respectively, and all calibration curves are fitted the second-order line using the sampled data. In **Figure 17**, with the relative pressure P/P_{ref} increasing, the relative luminous intensity I/I_{ref} is reduced under all settings of PSP measurement system, which is consistent with the PSP measurement principle. Compared with the calibration results using 200*W* UV lamp, sampled points using 400*W* is in order and have a good agreement with the fitted second-order calibration curve under all CCD apertures.

Calibration curves using 400*W* UV lamp is much steeper and keeps a better monotonic property.

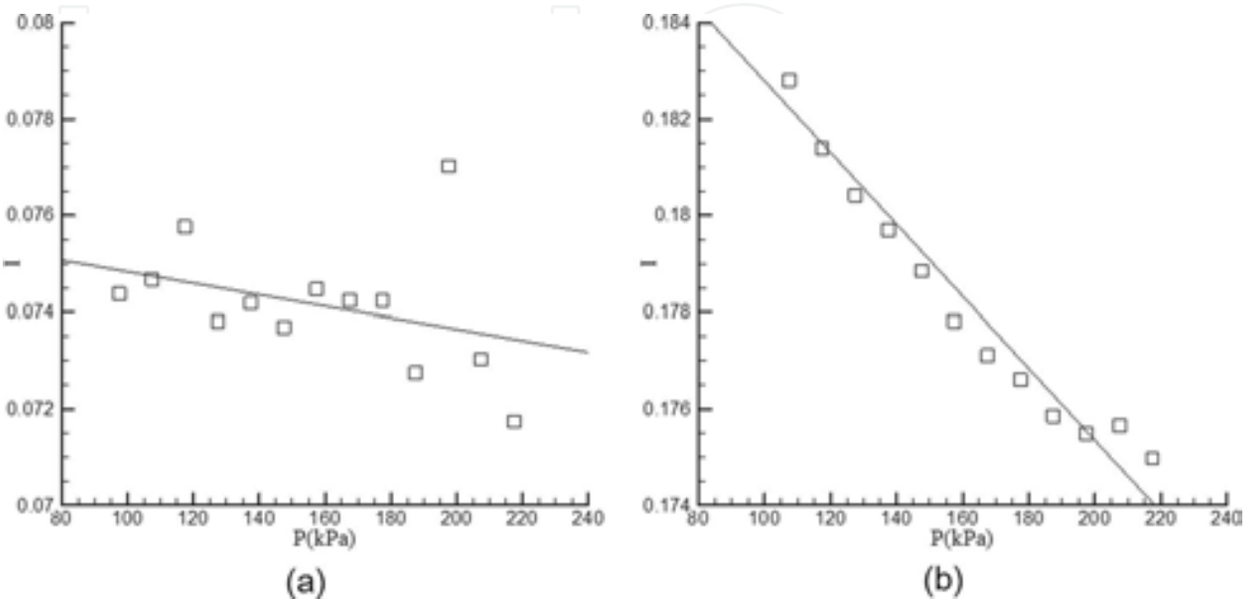

Figure 16. Luminous intensity frame using two powers of UV lamp. (a) 200W power; (b) 400W power.

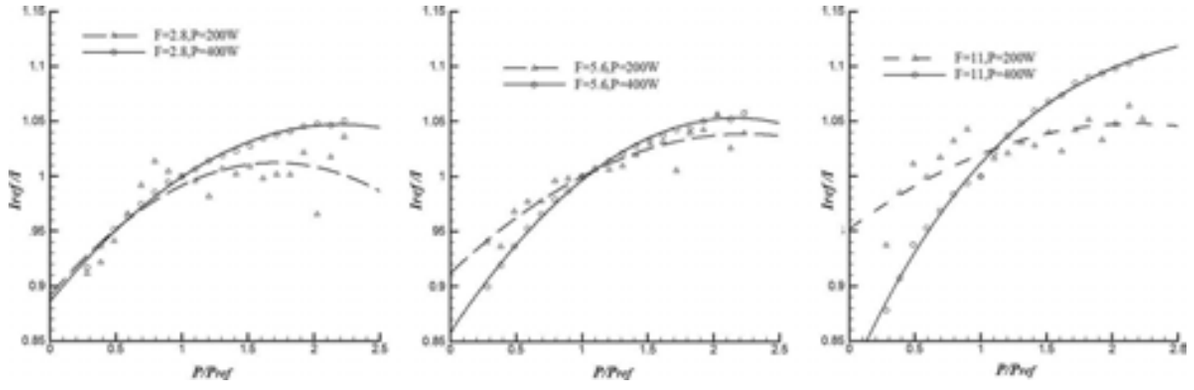

Figure 17. Calibration curve using two powers of UV lamp with typical apertures at 2.8 (a), 5.6 (b) and 11 (c).

4.2. Characteristics of camera aperture

It was also found from **Figure 17** that the setting of CCD aperture has an influence on the measured result. In the present study, the optimization of CCD aperture (2.8, 4.0, 5.6, 8 and 11) is performed with 400*W* UV lamp. Original PSP images are showed in **Figure 18** with two typical camera apertures: **Figure 18(a)** is with the aperture at 5.6 and **Figure 18(b)** with the

http://dx.doi.org/10.5772/64008

aperture at 11. Due to the oxygen quenching, it also can be seen from **Figure 18** that the image is darker and darker with the pressure increasing. Compared with **Figure 15(b)**, **Figure 18(a)** and **Figure 18(b)**, the original PSP image is getting darker with CCD aperture increasing under the same pressure and excitation light.

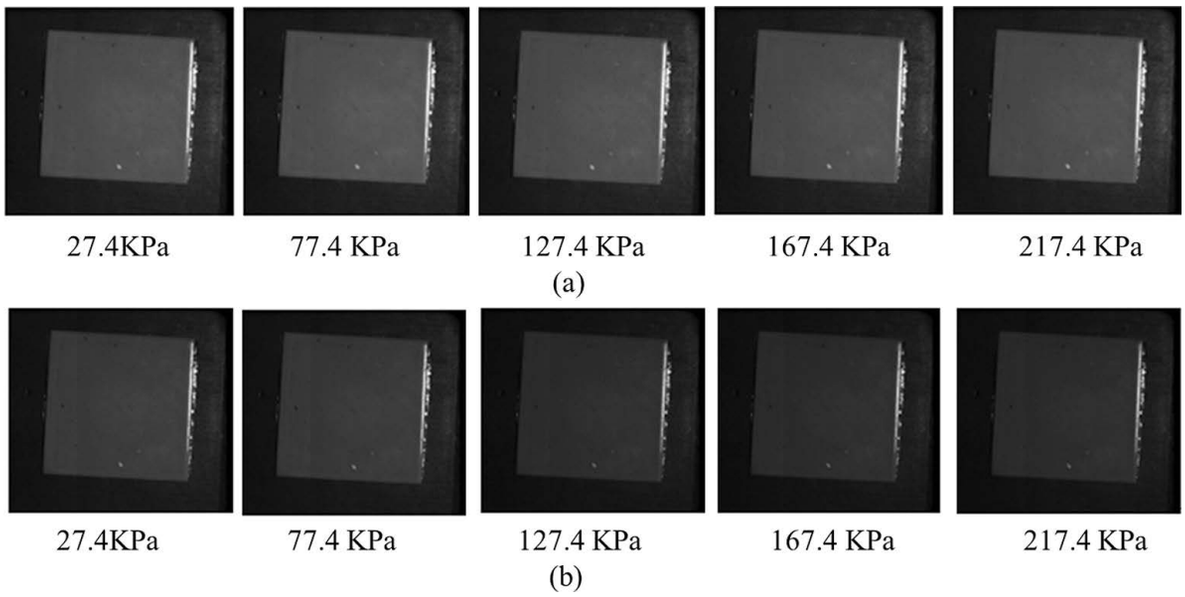

Figure 18. Images with typical CCD apertures at 5.6 (a) and 11 (b).

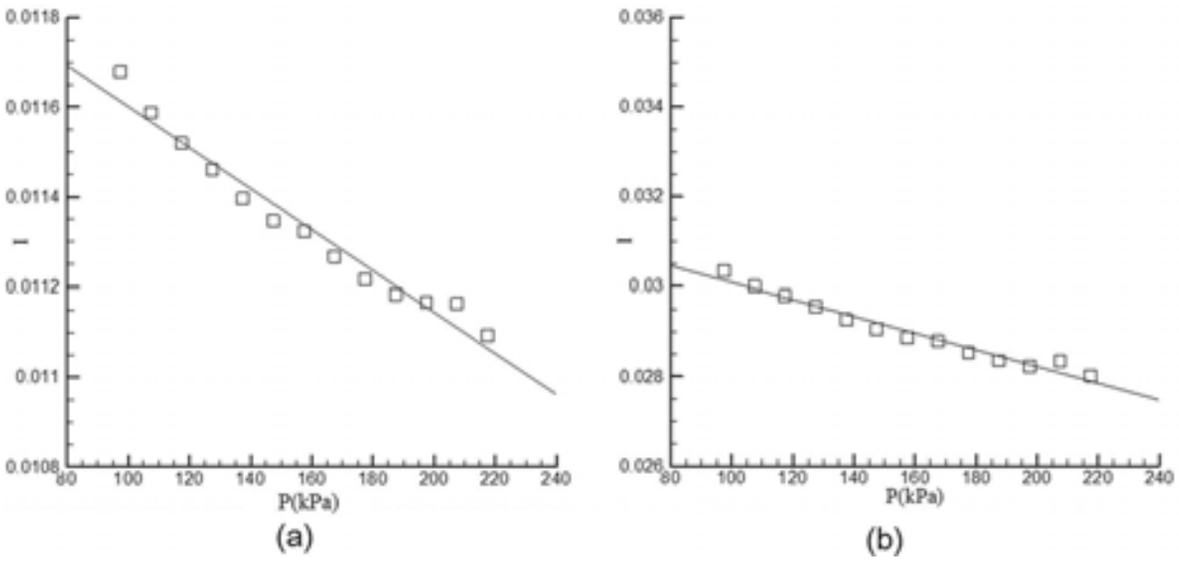

Figure 19. Luminous intensity frame with typical CCD aperture at 4 (a) and 8 (b).

To show the influence of the CCD apertures more clearly, the luminous intensity of the image is quantified using the grey value of the model surface centred point in **Figure 19**. Sampled data using different CCD apertures show higher linearity using the 400*W* UV lamp. However,

the luminous intensity in **Figure 19(b)** is obviously greater and changing sharper than that with 2.8 (see **Figure 16(b)**) and 4 (see **Figure 19(a)**), which corresponds to **Figure 18**. The main reason is that CCD lens captures more luminescence with the increasing CCD aperture and results in an increase in the grey scale of the PSP image.

All calibration curves with five CCD apertures are shown in **Figure 20**. The calibration curves are very close when the CCD aperture is set as 4 and 2.8. The calibration curve becomes steeper with the CCD aperture increasing and is nearly linear when CCD aperture is 11. Clearly, due to the improved SNR (Signal Noise Ratio) of CCD, the pressure calibration curve is mostly sensitive to the pressure change and keep better monotonic when the CCD aperture is 11, especially when the pressure is higher.

Figure 20. Calibration curve in different apertures.

http://dx.doi.org/10.5772/64008

5. Examples of optical PSP

5.1. Global pressure distribution on suction surface of a compressor cascade

5.1.1. Test rig

In the references [13–15], the two sets of PSP experiment are performed in a transonic cascade wind tunnel: one is based on the self-established PSP system, the other based on the commercial PSP system by ISSI. And the global pressure distributions on two sets of compressor blade are measured on several inflow conditions. Finally, PSP results are compared with that with the traditional measurement technique.

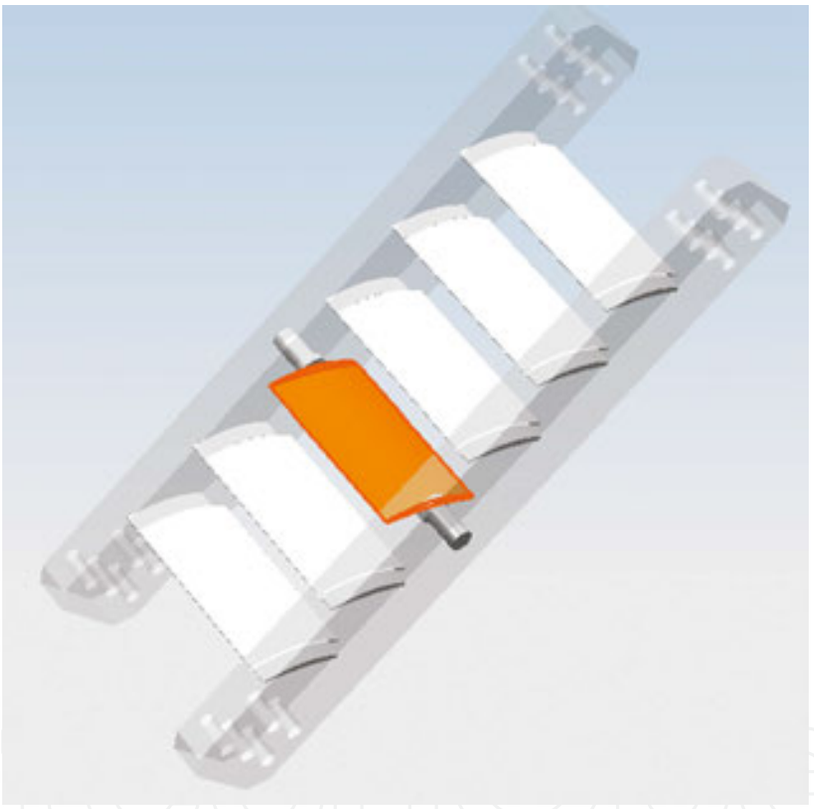

Figure 21. Schedule of cascade.

PSP experiments are carried out in the Science and Technology Key Lab's transonic cascade wind tunnel in Northwestern Polytechnical University (NPU). The experimental cascade is composed of several blades and two end-walls (see **Figure 21**). In the present work, two sets of the PSP measurement system are used: one is the own established PSP system by ourselves, and the other is the commercial PSP system produced by ISSI. Correspondingly, two sets of cascade are provided as the PSP measured model: blade1 is coated with PSP from ICAS (Institute of Chemistry, Chinese Academy of Science) in **Figure 22**, and blade2 iss coated with PSP from ISSI in **Figure 23**.

Figure 22. Blade 1 coated with ICAS PSP.

Figure 23. Blade 2 coated with ISSI PSP.

http://dx.doi.org/10.5772/64008

5.1.2. Result of blade 1

Based on the established measurement system, the pressure distribution on blade1, whose chord is 56.7 mm, bend angle is 52.6°, height is 100 mm, is measured under two conditions: Ma=0.4 and Ma=0.5. with the same incidence angle (i=−10°).

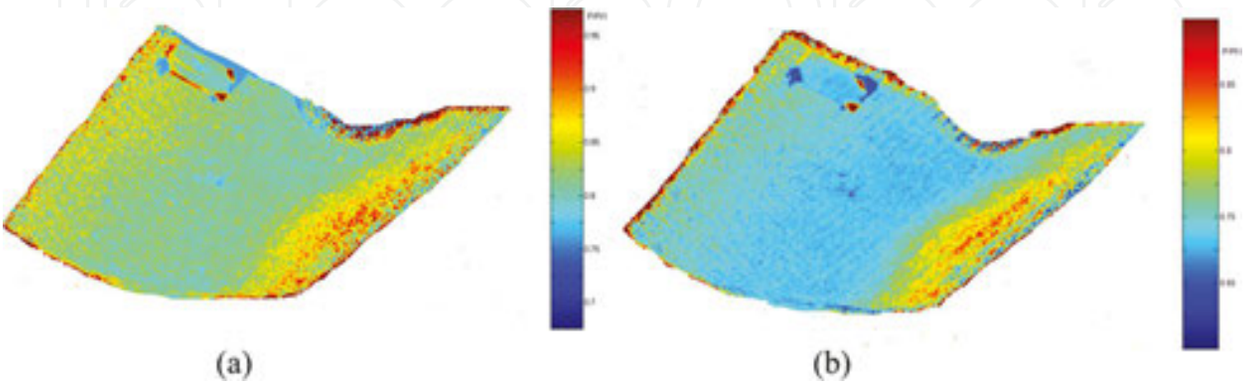

Figure 24. Static pressure distribution on suction surface at Mach 0.4 (a) and Mach 0.5 (b).

Figure 24 shows the pressure distribution on suction surface at Mach 0.4 and Mach 0.5 respectively. From two pressure map, there is a high pressure area near the leading edge. Under the action of the large negative attack angle and the larger pitch between two neighbourhood blades, the inflow injects onto the blade leading edge and decelerates quickly, consequently, the pressure increases. Then, airflow began accelerating and the pressure decreases because of the large curvature on blade surface. At 40% chord, airflow accelerated to max and a pressure valley is shown in the pressure map. Due to the divergence of the cascade passage, pressure grows up again. In addition, due to the boundary layer interfering mutually between end-wall and blade surface, pressure at the corner between the end-wall and blade surface is smaller than the other area.

Although there are two results at different Mach number in **Figure 24**, there is the same pressure distribution trend on suction surface, and the surface pressure is increasing with the rising inlet Mach number.

To test the measurement precision of PSP technique, the averaged-pressure around pressure holes is compared with the pressure measured by conventional pressure tap, and the results are shown in **Figure 25**. In the plot, X-coordinate shows the relative chord, Y-coordinate shows dimensionless pressure.

From **Figure 25**, it is seen that the pressures measured by PSP technique and pressure tap follow the same trend in two different conditions. The position of the lowest pressure on blade suction surface coincided nearly. The pressure error at the same position is less than 4.5%, which meets the engineering application basically.

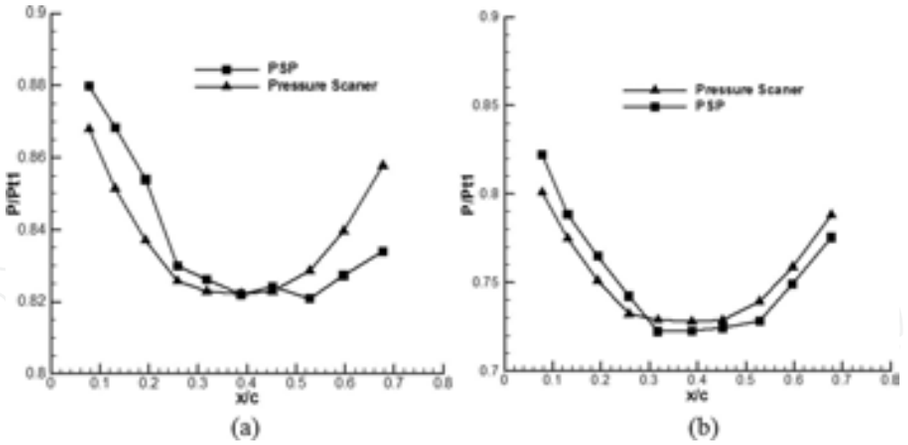

Figure 25. Pressure on the 50% span at Mach 0.4 (a) and Mach 0.5 (b) using PSP and pressure scanner.

5.1.3. Result of blade 2

Based on the ISSI PSP system, the pressure distribution on blade 2, whose chord is 69.946 mm, pitch is 60.7 mm, height is 100 mm, is measured using ISSI PSP under three conditions: Ma=0.4, 0.5 and 0.6 with the same incidence angle (i=0°).

Figure 26 shows the pressure distribution on suction surface at Mach 0.4, 0.5 and 0.6 respectively. It shows that the distribution of pressure in different conditions has almost the same trend. While with the increase of the inlet Mach, the pressure at the same position decreases. Similar to the blade 1 results, the pressure at the corner of blade 2 between the end-wall and blade surface is smaller than the other area due to the boundary layer interfering. Besides, the pressure increases along the blade chord due to the divergence of the cascade passage.

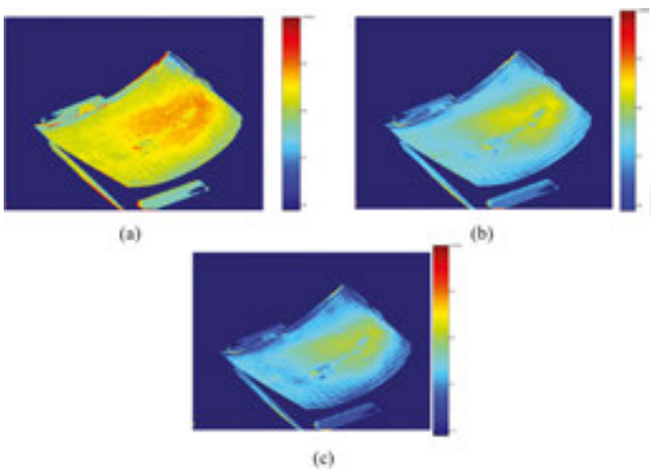

Figure 26. Static pressure distribution on suction surface at Mach 0.4 (a), 0.5 (b) and 0.6 (c).

To test the measurement precision of PSP technique, the averaged-pressure around pressure holes is compared with the pressure measured by conventional pressure tap, and the results

http://dx.doi.org/10.5772/64008

are shown in **Figure 27**. In the plot, X-coordinate shows the relative chord, and Y-coordinate shows dimensionless pressure.

From **Figure 27**, it is seen that PSP measurement results have the same pressure distribution trend to the pressure scanner results on the two conditions. The position of the lowest pressure on blade suction surface coincided nearly. The pressure error at the same position is less than 4.5%, which meets the engineering application basically.

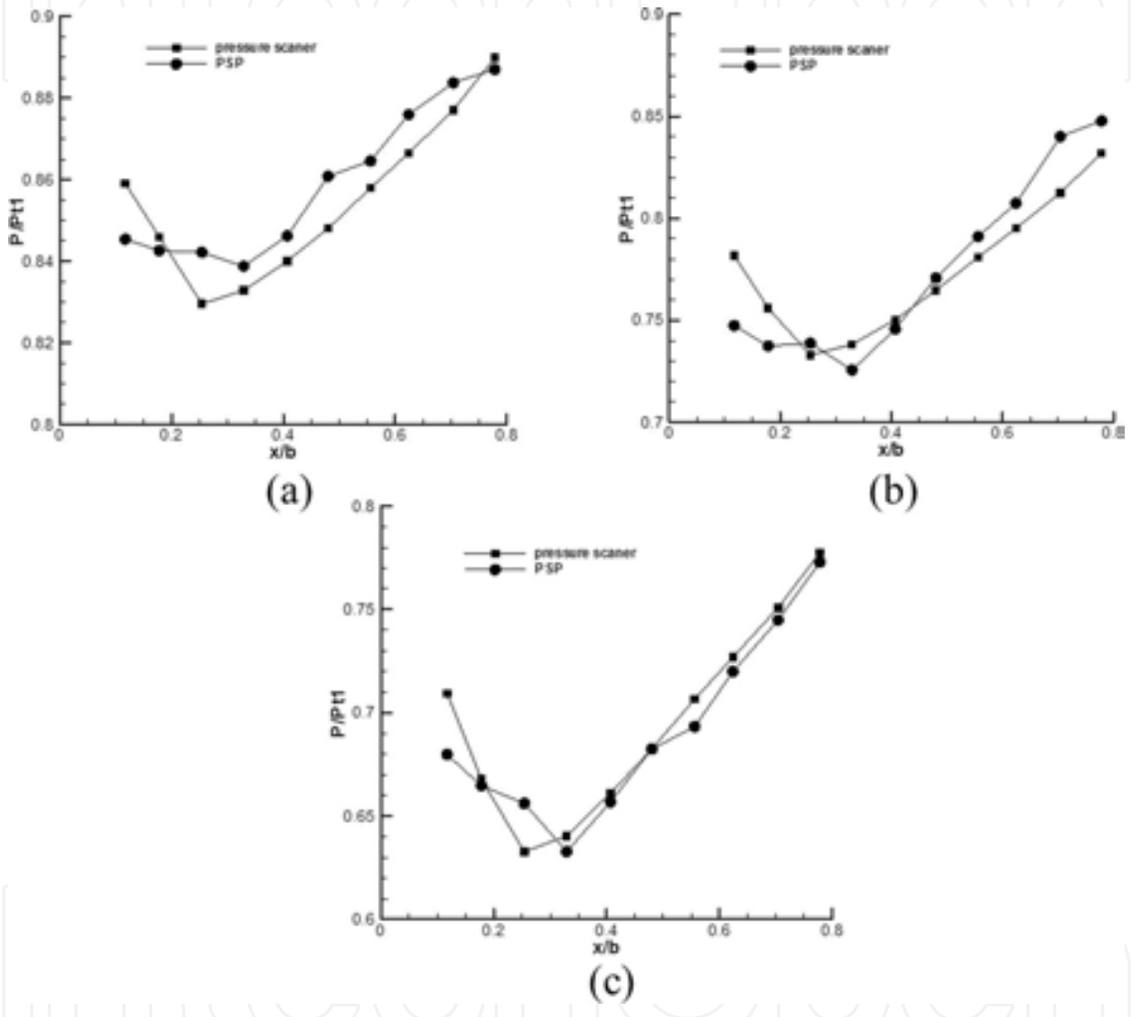

Figure 27. Pressure on the 50% span at Mach 0.4 (a), 0.5 (b) and 0.6 (c) using PSP and pressure scanner.

6. Conclusion

Pressure Sensitive Paint measurement technique is attracting extensive attention for its unique advantage at surface pressure measurement, such as the absence of intruding measured surfaces, application of image processing to acquire global pressure distribution, and the acquisition of PSP results that traditional methods could never obtain. In this chapter, both the

theory and application of PSP technique are introduced, including the measurement principle, measurement system, component characteristics and its application in internal flow fields based on author's researches. The results are proposed for engineering application.

Acknowledgements

This work was supported by the National Nature Science Foundation of China (NSFC) under the Grand No.51476132. Besides, Dr. Zhou Qiang was acknowledged for his valuable suggestion.

Author details

Limin Gao*, Ruiyu Li and Bo Liu

*Address all correspondence to: gaolm@nwpu.edu.cn

Northwestern Polytechnical University, Xi'an, PR China

References

[1] Ardasheva M. M., Nevskii L. B., Pervushin G. E. Measurement of pressure distribution by means of indicator coating. Journal of Applied Mechanics and Technical Physics 1985; 26(4):469–474. DOI: 10.1007/BF01101626.

[2] Radchenko V. N. Application of the luminescence in aerodynamic researches [thesis]. Zhokovsky: Moscow Physical-Technical Institute; 1985.

[3] Lepicovsky J., Bencic T. Use of pressure-sensitive paint for diagnostics in turbomachinery flows with shocks. Experiments in Fluids. 2002;33(4):531–538. DOI: 10.1007/s00348-002-0476-x.

[4] Watkins A. N., Goad W. K., Obara C. J., Danny R. S., Richard L. C., Melissa B. C. Flow visualization at cryogenic conditions using a modified pressure-sensitive paint approach. In: 43rd AIAA Aerospace Sciences Meeting and Exhibit; 10–13 January; Reno, Nevada. AIAA; 2005. 456.1–456.13.

[5] Erickson G. E., Gonzalez H. A. Pressure-sensitive paint investigation of double delta wing vortex flow manipulation. In: 43rd AIAA Aerospace Sciences Meeting and Exhibit; 10–13 January; Reno, Nevada. AIAA; 2005. 1059.1–1059.59.

[6] Gouterman M. Oxygen quenching of luminescence of pressure-sensitive paint for wind tunnel research. Journal of Chemical Education. 1997;74(6):697–704. DOI: 10.1021/ed074p697.

[7] Morris M. J., Donovan J. F., Kegelman J. T., Schwab S. D., Levy R. L. Aerodynamic applications of pressure sensitive paint. AIAA Journal. 1993;31(3):419–425. DOI: 10.2514/3.11346

[8] Wu Y. N. Application of pressure sensitive paint in internal flows [thesis]. Xi'an, PR China: Northwestern Polytechnical University; 2014.

[9] Wu Y. N., Gao L. M., Xie J., Liu B. Application in PSP measurement on blade's surface for image 3D reconstruction. In: Proceedings of AJCPP2012; 1–4 March; Xi'an, China. 2012. p. 138.1–1238.5.

[10] Gao L. M., Gao J., Xie J., Liu B. Application of image 3D reconstruction to pressure measurement on blade surface. Journal of Engineering Thermophysics. 2012;33(9): 1523–1526.

[11] Zhou Q., Liu B., Gao L. M., Chen L. S., Shi M. Pressure measurement on suction surface of a single vane using pressure-sensitive paint. Chinese Journal of Aeronautics. 2009;22(2):138–144. DOI: 10.1016/S1000-9361(08)60079-5.

[12] Gao L. M., Wang H., Han W., Liu B., Zhou Q. Experimental of study influence of measurement system characteristics on pressure-sensitive calibration. Acta Aeronautica et Astronautica Sinica. 2010;31(1):76–81.

[13] Wang H. Pressure sensitive paint technique in compressor cascade experiment [thesis]. Xi'an, PR China: Northwestern Polytechnical University; 2010.

[14] Gao L. M., Gao J., Wang H., Zhou Q., Liu B. PSP experiment of global surface pressure distribution on suction surface of compressor cascade with large curved angle. Journal of Aerospace Power. 2011;26(9):2061–2067.

[15] Gao L. M., Gao J., Wang H., Liu B., Zhou Q. Application of PSP technique to pressure measurement on cascade surface. Journal of Engineering Thermophysics. 2011;32(3): 411–414.

IntechOpen